Methods in Cell Biology

Prepared under the Auspices of the American Society for Cell Biology

VOLUME 63

Cytometry
Third Edition, Part A

Edited by

Zbigniew Darzynkiewicz

Brander Cancer Research Institute
New York Medical College
Hawthorne, New York

Harry A. Crissman

Cell and Molecular Biology Group
Los Alamos National Laboratory
Los Alamos, New Mexico

J. Paul Robinson

Purdue Cytometry Laboratories
Purdue University
West Lafayette, Indiana

CHAPTER 27

Three-Dimensional Imaging of Extracellular Matrix and Extracellular Matrix–Cell Interactions

Sherry L. Voytik-Harbin,[*,†] Bartlomiej Rajwa,[‡] and J. Paul Robinson[*,†]

[*]Department of Basic Medical Sciences
School of Veterinary Medicine; and

[†]Department of Biomedical Engineering
Purdue University
West Lafayette, Indiana 47907

[‡]Department of Biophysics
Institute of Molecular Biology
Jagiellonian University
31-120 Krakow, Poland

I. Introduction

In tissues, cells reside within a complex, three-dimensional (3-D) assembly of collagens, proteoglycans, glycosaminoglycans, and glycoproteins, otherwise

known as the extracellular matrix (ECM). Reciprocal communication between cells and their ECM plays an important role in the modulation of critical physiological and pathological processes, including acquisition and maintenance of differentiated phenotypes during embryogenesis, the development of form (morphogenesis), vessel formation (angiogenesis), wound healing, and even tumor metastasis (Bissell *et al.*, 1982). A major challenge to the biomedical community is to further understand the biophysical and biochemical aspects of ECM assembly and signaling as it relates to the structure and function of tissues and organs. One goal of our laboratory is to develop and identify approaches to visualize and quantitate the dynamic processes of the ECM and its interaction with cells within complex, 3-D, living biological systems. Herein we describe the integration of the principles and practices of microscopy with those of cell and extracellular matrix biology.

II. Three-Dimensional Imaging of Extracellular Matrix and Extracellular Matrix–Cell Interactions: Current Techniques and Their Limitations

Knowledge of the spatial distribution of biological components within cells and tissues often provides insight to their function and basic mechanisms of action. Unfortunately, many imaging techniques are either unable to provide insight into 3-D preparations or demand efforts that are often prohibitive to observations within living systems.

A. Light Microscopy

Light microscopy has been used routinely in conjunction with histochemical methods to visualize the components of cells, ECM, and tissues. Unfortunately, high quality images are often limited to thin, physically sectioned specimens or two-dimensional (2-D) culture systems in which cells grow along a translucent substrate (e.g., plastic). Thick slices or whole mount specimens cannot be readily studied because structures in the interior of the specimen are obscured by interferences from structures above and below the plane of focus. Although a third dimension can be reconstructed from hundreds of 2-D images generated from serial sections, this process is lengthy and tedious, and accurate image alignment is difficult. Likewise, physical sectioning requires extensive specimen processing including fixation, dehydration, and embedding, rendering this method inappropriate for viewing living systems. An alternative method for obtaining 3-D information involves recording a series of images within adjacent focal planes. Image degradation due to low-resolution "out-of-focus" light is then corrected by computer-based image processing known as deconvolution (for review, see Shaw, 1995). From a practical point of view, the major problems with deconvolution

include the significant computing time and disk space needed for image processing as well as knowledge of an accurate point spread function. The latter requirement may be eliminated when so-called blind deconvolution is applied (Holmes *et al.,* 1995). Deconvolution computations can take from minutes to days, depending on the size of the image and the algorithm, computer, or number of iterations used.

B. Electron Microscopy

Electron microscopy (EM) uses a beam of electrons to form an image of a specimen. While offering much improved resolution, electron microscopy requires extensive specimen processing due to electron beam observation in vacuum. In fact, there is no real possibility of viewing biological specimens in a living, wet state, owing to the high vacuum operation of EM. Because of the very limited penetrating power of electrons, observations by transmission electron microscopy (TEM) require specimens that are cut into extremely thin sections before they can be viewed. As with light microscopy, EM visualization of samples in three dimensions can be achieved by collecting and aligning information gathered from a large number of serial sections. Alternatively, thick specimens may be imaged at two different tilt angles and viewed as a stereopair with a stereoviewer for purposes of 3-D visualization only. More recently, 3-D volume reconstruction of EM images has been achieved by electron tomography (Frank, 1992). This technique involves incrementally tilting the specimen through a range of angles, usually about 60°, and then backprojecting each of the tilt images.

In contrast, scanning electron microscopy (SEM) involves scanning the specimen with a very narrow beam of electrons and collecting the electrons scattered or emitted from the surface of the specimen. Since the amount of electron scattering depends on the angle of the surface relative to the beam, the SEM image has highlights and shadows and gives a 3-D appearance. Preparing samples for SEM usually requires fixation, dehydration, and drying whether by the critical point method or by freeze-drying. More recently, less well-known cryopreparation techniques have been used to preserve the native detail of biological structures, especially those with significant water content, with a high degree of fidelity and fewer artifacts (Voytik-Harbin *et al.,* 1998a).

Indeed, electron microscopy has been instrumental in elucidating the structural organization and binding interactions of individual protein and proteoglycan components of the ECM (for reviews, see Engel and Furthmayr, 1987; Engel, 1994). Despite the obvious advantages in resolution, these techniques do not provide true 3-D images and have been mostly limited to simple, nonliving systems often involving purified or partially purified ECM preparations.

C. Confocal Microscopy

Since the advent of confocal microscopy in the mid-1980s, 3-D spatial information can be collected from thick specimens by means of optical sectioning. The

term confocal is derived from the optical platform in which the scanning point light source and the detector aperture share a common focus at the level of the specimen. This optical arrangement effectively eliminates much of the out-of-focus light from detection, thus improving the fidelity of focal sectioning in three dimensions (Sheppard, 1987; Wijnaendts van Resandt *et al.,* 1985). This technology offers the principal advantages of (1) thin optical "slices" through thick specimens, (2) rejection of out-of-focus light from other focal places, and (3) resolution in all three dimensions from multiple optical slices. This instrument faithfully images structures with dimensions as small as subcellular organelles up to whole tissue preparations (Brakenhoff *et al.,* 1979, 1988; Messerli and Perriard, 1995). However, a variety of technical constraints limit the maximal thickness of the objects that can be imaged. To obtain 3-D images that closely represent the geometry of the sample, the light path through the sample must be as short as possible, since imaging artifacts like astigmatism, spherical aberration, and intensity attenuation increase with path length (Aslund and Liljeborg, 1992; Hell *et al.,* 1993; Visser *et al.,* 1991). Coupled with digital reconstruction techniques, confocal microscopy can extract image information that, while present in the data, is not easily accessible by simply presenting the individual sections.

D. Multiphoton Microscopy

Three-dimensional optical sectioning is also possible with multiphoton microscopy. This technology, developed in 1989 (Denk *et al.,* 1990), is based on a well-known quantum mechanical concept presented for the first time by Maria Goeppert-Mayer in 1931. Specifically stated, multiphoton refers to the effect of two or three photons in a single quantum event (Goeppert-Mayer, 1931). This phenomenon allows two or more photons of long wavelength light to create the same excitation as one photon of shorter wavelength light provided the photons arrive simultaneously (Denk *et al.,* 1990). Several clear distinctions exist on comparison of confocal and multiphoton imaging technologies. These distinctions should be carefully considered when deciding which technology is most suited to a specific microscopic application. With multiphoton microscopy, the power density of the laser is only high enough to excite fluorescence in the focal volume. Therefore, unlike confocal microscopy, a pinhole aperture is not needed to exclude unwanted light. The elimination of the aperture results in an increase in the overall signal intensity detected with the multiphoton system. Because multiphoton excitation is restricted to a small focal volume, out-of-focus photo-damage and photobleaching are almost eliminated. However, the longer wavelength source used in multiphoton excitation can have some potential drawbacks: system resolution will be less than a comparable laser scanning confocal system, the ultrashort pulsed source may also potentially excite intrinsic absorption in cells via two- and three-photon excitation, and sample heating may be a concern for excitation wavelengths near 1 μm (Wokosin *et al.,* 1996). A potential advan-

tage of multiphoton microscopy is the increased tissue depth and the reduced damage at wavelengths in the ultraviolet (UV) range (Potter, 1996).

III. Three-Dimensional Microscopy of Living Systems: Extracellular Matrix and Extracellular Matrix–Cell Interactions

A. Reflected Light Imaging

1. Introduction

Reflected or back-scattered light is an intrinsic optical property of many materials that can be exploited to provide qualitative and quantitative microstructural information. When used in this mode, confocal microscopy, can provide 3-D structural details of unfixed and unstained biological specimens (Boyde and Jones, 1995). For example, Semler and co-workers applied confocal reflection microscopy (CRM) to visualize and quantitate the microtopography of porous biomaterials prepared from synthetic polymers (Semler *et al.*, 1997). Likewise, we and others have applied this technique for surface and volume visualization of intact ECM biomaterials as well as 3-D reconstituted matrices consisting of individual (e.g., collagen) or mixtures of ECM components (Gunzer *et al.*, 1997; Friedl *et al.*, 1997; Brightman *et al.*, 2000). Reflected light from collagen fibers has been collected simultaneously with fluorescence from cells stained with vital fluorochromes to monitor the dynamic process of cell migration through a 3-D collagen matrix (Friedl *et al.*, 1997). More recently, we have provided the first account of CRM in a time-lapse mode for studying collagen fiber formation (fibrillogenesis) and ECM assembly *in vitro* (Voytik-Harbin *et al.*, 1998b; Robinson *et al.*, 1999; Brightman *et al.*, 2000).

With time-lapse CRM both kinetic and 3-D structural information can be collected simultaneously as ECM components polymerize from a soluble to a gel phase. Taken together, CRM offers a useful technique for investigating biological processes in living systems involving the ECM and ECM–cell interactions that occur in multiple dimensions. Examples of such complex events include collagen fibrillogenesis, ECM assembly, morphogenesis, and cell migration. A detailed description of the application of CRM for visualization and analysis of collagen fibrillogenesis and ECM assembly is provided herein.

2. Methods

A soluble form of purified type I collagen, Vitrogen, was obtained from Collagen Aesthetics (Palo Alto, CA). *Solubilized mixtures of ECM components were prepared from small intestinal submucosa, an intact interstitial ECM, as described previously (Voytik-Harbin et al., 1998a).*

Unstained 3-D matrices of type I collagen or mixtures of ECM components were polymerized in Lab-Tek chambered coverglass (Nalge Nunc Int, Rochester, NY) and imaged using a Bio-Rad MRC1024 confocal microscope via a 60×, 1.4 NA (numerical aperature) oil immersion lens. Optical settings were established and optimized on reconstituted matrices after polymerization was completed. An aliquot of soluble collagen or ECM preparations then was placed onto the heated (37°C) stage of the microscope and fibrillogenesis and fibril assembly imaged. Samples were illuminated with 488 nm laser light, and the reflected light was detected with a photomultiplier tube (PMT) using a blue reflection filter. For the Bio-Rad MRC1024 confocal microscope, instrument setup involved a beam splitter placed in position D1 and a dichroic filter that reflects 488 nm light into PMT2 in position D2 (Fig. 1). Optical filters can be added in positions W1 and W3 for the simultaneous collection of fluorescence
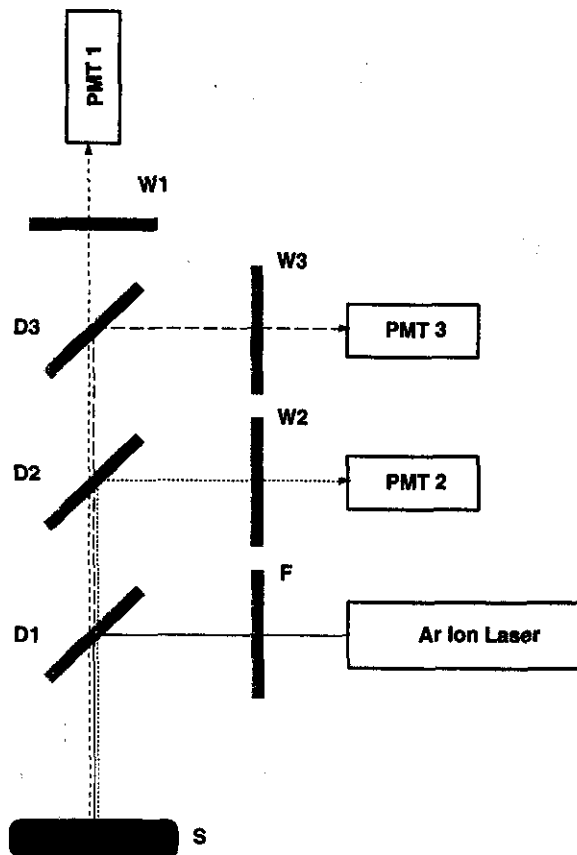
Fig. 1 Confocal microscope demonstrating filter (D, W, and F) and photomultiplier tube (PMT) positions.

information in PMT1 and PMT3, respectively. A z-step of 0.2 μm was used to optically section the samples. Because the resolution of the z-plane is less than that of the x–y plane, the sampling along the z-axis may be different from that of the x–y plane. 2-D (e.g., x–y) or 3-D (e.g., x–y–z) sections demonstrating fibrillogenesis and assembly events were recorded at step intervals ranging from 1 to 5 sec for up 1 hr. Minimum time intervals required for image collection are dependent on the section size, resolution, and scanning mode (point versus line). For standardization of scanning depth, the scan head was adjusted to a distance in the range of 20–50 μm from the upper surface of the coverglass.

Nonuniform background caused by interference and reflection from the optical pathway was removed from the images using a standard rank leveling procedure on each x–y section. Rank leveling consists of applying a multiple number of erosions followed by a Gaussian filter to each section to create a background approximation. This background approximation was then subtracted from the original section to enhance the signal to noise ratio. Three-dimensional images of reconstituted ECM biomaterials were either compiled into a single view projection using Laser Sharp image processing software (Bio-Rad, Hemel Hempstead, England) or compiled into a 3-D projection using Voxel-View reconstruction software (Vital Images, Minneapolis, MN). Rank leveling can also be performed on 3-D images prior to reconstruction into 3-D views to improve image quality. To perform rank leveling in two dimensions we used public domain Unix image processing toolsets: "imgstar" by Simon Winder and "pbmplus" by Jef Poskanzer. A "tcsh" script was used to automate the image processing tasks. Time-lapse image files were assembled into SGI movie format (sgimv) or MPEG movie format using "dmcovert," a standard converter for digital media, a part of the Irix 6.2 operating system on a Silicon Graphics Indigo2 workstation (SGI, Mountain View, CA). Because MPEG movie formatting involves lossy compression, this format was used only for visualization purposes.

3. Results

Confocal reflection images from unfixed, unstained 3-D matrices prepared from purified collagen or mixtures of ECM components revealed the morphology of individual fibrils as well as their density and orientation within the 3-D matrix (Fig. 2). Results obtained with CRM confirmed the dependence of matrix structure on composition as previously documented using SEM (Voytik-Harbin *et al.*, 1998a). Initial quantitative analyses of collagen matrices with CRM indicate fiber diameters ranging from 200 to 600 nm. These results are similar to those reported by Friedl using the same technique (Friedl *et al.*, 1997). For matrices prepared using air-drying and standard critical point drying techniques and visualized using SEM, average fiber diameters were significantly diminished and architectural discrepancies noted (Friedl *et al.*, 1997; Voytik-Harbin *et al.*, 1998a). Only with cryostage SEM, in which the specimen is viewed in a quick-frozen hydrated state, were fiber diameters similar to those observed with CRM. For
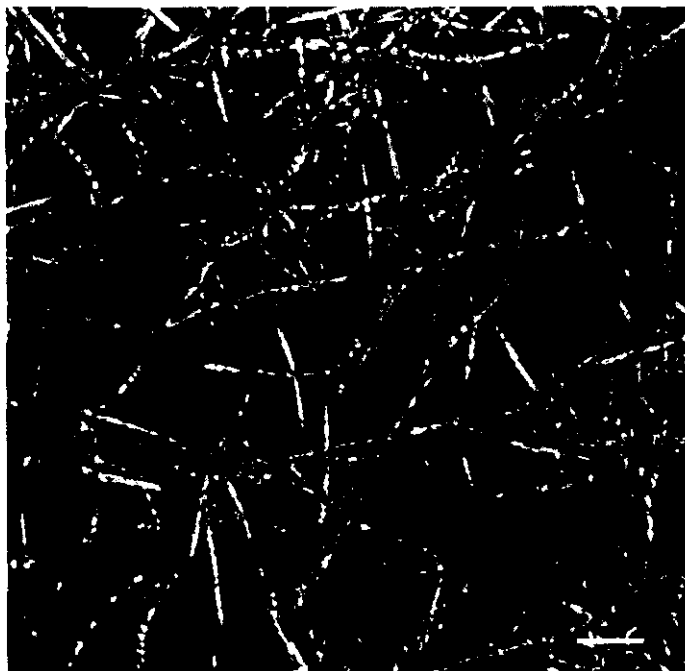
Fig. 2 Confocal reflection image of reconstituted 3-D matrix prepared from type I collagen (1.5 mg/ml). Scale bar = 5 μm.

reconstituted or intact ECM biomaterials, the depth resolution was inversely related to specimen opacity. For the intact ECM, intestinal submucosa, surface topography and depths of 10–20 μm could be effectively imaged with CRM without difficulty.

To date, spectrometry and dark-field microscopy techniques have been used for investigations of collagen fibrillogenesis and ECM assembly. Although these routine techniques provide either structural or kinetic information only, CRM allowed the collection of both types of data simultaneously. Time-lapse imaging of fibril polymerization and assembly demonstrated the dependence of kinetic parameters as well as architecture on matrix composition. For example, the addition of heparin to purified type I collagen or the complex ECM mixture resulted in an increase in the assembly (fibrillogenesis) rate, an increase in fibril thickness, and a decrease in fibril length. On the other hand, the addition of the proteoglycan decorin increased the lag phase and reduced the rate of collagen fibrillogenesis.

As with fluorescence-based imaging, CRM is a very sensitive technique. It benefits from the fact that although some very small reflecting particles or fibrils cannot be resolved (according to the Rayleigh criterion), they still can be detected

and visualized. Based on the Rayleigh criterion, the calculated resolution for our CRM system was 212 nm. Interestingly, the $x-y$ resolution of a microscope operating in reflected light mode is not improved by the confocal iris, but the contrast transfer characteristics for fine detail are much better than in the case of a nonconfocal microscope (Oldenbourg *et al.*, 1993). In these studies, optimized fiber contrast scanning distances ranged from 20 to 50 μm from the coverslip. Depth intensity of the fiber contrast was diminished at deeper focus levels, indicating substantial scattering and refraction of the laser intensity. Although offering resolution that is significantly less than that of SEM (2–8 nm), CRM readily provided 3-D spatial information and did not require extensive processing techniques (e.g., physical sectioning and staining). High throughput computer algorithms for quantitation of various fibril and matrix parameters, including diameter, length, degree of curvature, and orientation within the matrix, are currently under development.

B. Autofluorescence

1. Introduction

In the application of fluorescence and histochemical staining methods for microscopic investigation of ECM–cell interactions within *in vivo* and *in vitro* model systems, background autofluorescence has been observed and often deemed problematic. The autofluorescence has been attributed to naturally oc-curring fluorophores such as the prominent ECM components collagen and elastin. This autofluorescence represents the superposition of multiple intrinsic fluorophores within the ECM and is also dependent on the light absorption and scattering properties of the ECM. However, it should be noted that the physical environment, including pH, solvation, and oxidation state, affects the fluorescent properties of these molecules. Since the 1980s, characterization of tissue fluores-cence in terms of the native fluorophores has been proposed as a method of differentiating between normal and diseased tissues (Schomacker *et al.*, 1992; Brennan, 1989; Deckelbaum *et al.*, 1987) as well as of studying the effect of aging (Kollias *et al.*, 1998; Leffell *et al.*, 1988). For these purposes, measurements have been conducted on solubilized or intact tissue specimens using standard spectrofluorometric or fiber optic systems. Here we describe the collection of autofluorescence from intact ECM biomaterials as well as 3-D tissue culture systems for the study of ECM architecture and ECM–cell interactions. Autofluo-rescence is an ideal optical property for visualization because it essentially re-quires no sample preparation and processing. When used in conjunction with vital dyes for cells, autofluorescence is an effective tool for investigating ECM–cell interactions in 3-D, living biological systems.

2. Methods

The intact ECM biomaterial, small intestinal submucosa (SIS), was obtained from Cook Biotech (West Lafayette, IN). This same biomaterial was used as a

3-D ECM substrate for the culture of human coronary artery smooth muscle cells *in vitro* as previously described (Voytik-Harbin *et al.*, 1998a; Sturgis *et al.*, 1998).

Confocal imaging of autofluorescence was performed on a Bio-Rad MRC1024 confocal microscope. The microscope was adapted with a dichroic filter that reflects 488 nm and passes all wavelengths greater than 520 nm in position D1 (UBHS, Bio-Rad) and with a dichroic filter that directed fluorescence to PMT2 in position D2. An argon ion laser was used to provide 488 nm excitation. To image ECM autofluorescence and fluorescence-labeled cells simultaneously, we equipped the Bio-Rad microscope with a dichroic mirror reflecting UV and 488 nm light in position D1 and a second dichroic in position D2 that split blue Hoechst 33342 fluorescence and yellow-green autofluorescence into PMT2 and PMT1, respectively.

For multiphoton autofluorescence imaging, an all-solid-state 1047-nm Nd:YLF laser (Microlase, Strathclyde, UK) and modified MRC-600 scan head (Bio-Rad, Hemel Hempstead, England) were configured as described previously (Wokosin *et al.*, 1996; Wokosin and White, 1997). The emission was detected by a standard S-20 PMT (Thorn 9828B, Electron Tubes, Rockaway, NJ) mounted external to the scan head directly beneath the objective of the microscope (direct detection).

3. Results

Autofluorescence imaging revealed the overall 3-D organization of collagen fibrils and bundles that form the structural backbone of intestinal submucosa (Figs. 3 and 4). Low intensity ECM autofluorescence could be collected with a confocal microscope over a broad range of UV and visible excitation wavelengths. For purposes of imaging 3-D culture systems consisting of ECM and cells, the vital dye Hoechst 33342 was used (Fig. 5). Hoechst 33342-labeled cells could be imaged with little or no detection of ECM autofluorescence with UV excitation. Likewise, excitation with visible 488 nm light was effective for imaging ECM autofluorescence, providing simultaneous collection of architectural details of the ECM.

Although high quality images could be obtained with both confocal and multiphoton excitation, the imaging penetration depth obtained with multiphoton microscopy and direct detection was greater than that obtained with confocal microscopy, as expected. This observation is consistent with those of Centonze and co-workers who reported that there was at least a twofold improvement in the maximum imaging penetration depth obtained with multiphoton excitation relative to confocal microscopy on a variety of biological samples (Centonze and White, 1998). The use of direct detection rather than signal collection followed by descanning likely contributed to improving the signal-to-noise ratio of the image, which in turn further increased the depth at which usable images could be obtained. The resolution of autofluorescence images compared to those based on fluorescence or reflected light was diminished. This reduction in resolution can be attributed to the use of longer wavelengths as well as to the low signal-
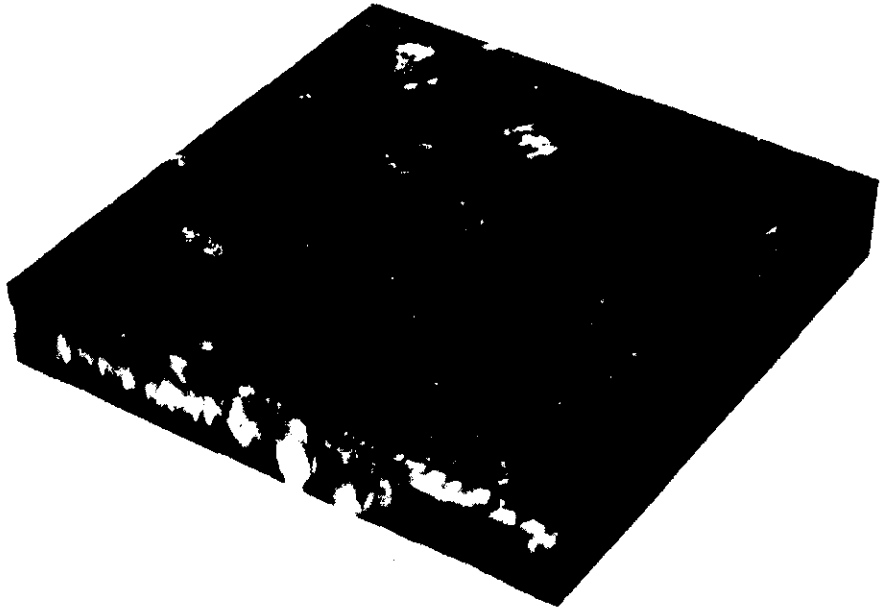
Fig. 3   3-D reconstructed confocal image demonstrating autofluorescence of a tissue-derived ECM biomaterial, small intestinal submucosa.

to-noise ratio characteristic of ECM autofluorescence. However, the relatively low signal provided by ECM autofluorescence provided an ideal background when imaging fluorescence-labeled cells on or within the intestinal submucosa substrate.

IV. Summary

In summary, noninvasive and nondestructive imaging modalities such as reflection and autofluorescence can readily be used in conjunction with the 3-D optical sectioning capabilities of confocal and multiphoton microscopy to investigate biological processes within living systems. The elimination of specimen fixation and extensive processing reduces the possibility of structural artifacts and facilitates repeat observations within a single sample. Therefore, information representing up to four dimensions (x, y, z, and time) can be readily collected and reconstructed for purposes of visualization and/or quantitative analysis. An advantage of using the techniques described in this chapter is the possibility of performing quantitative measurement of cell size, surface area, volume, depth (in matrix), orientation, receptor density, as well as fluorescence-based indicators of phenotype and function. At present, we are effectively utilizing these tech-
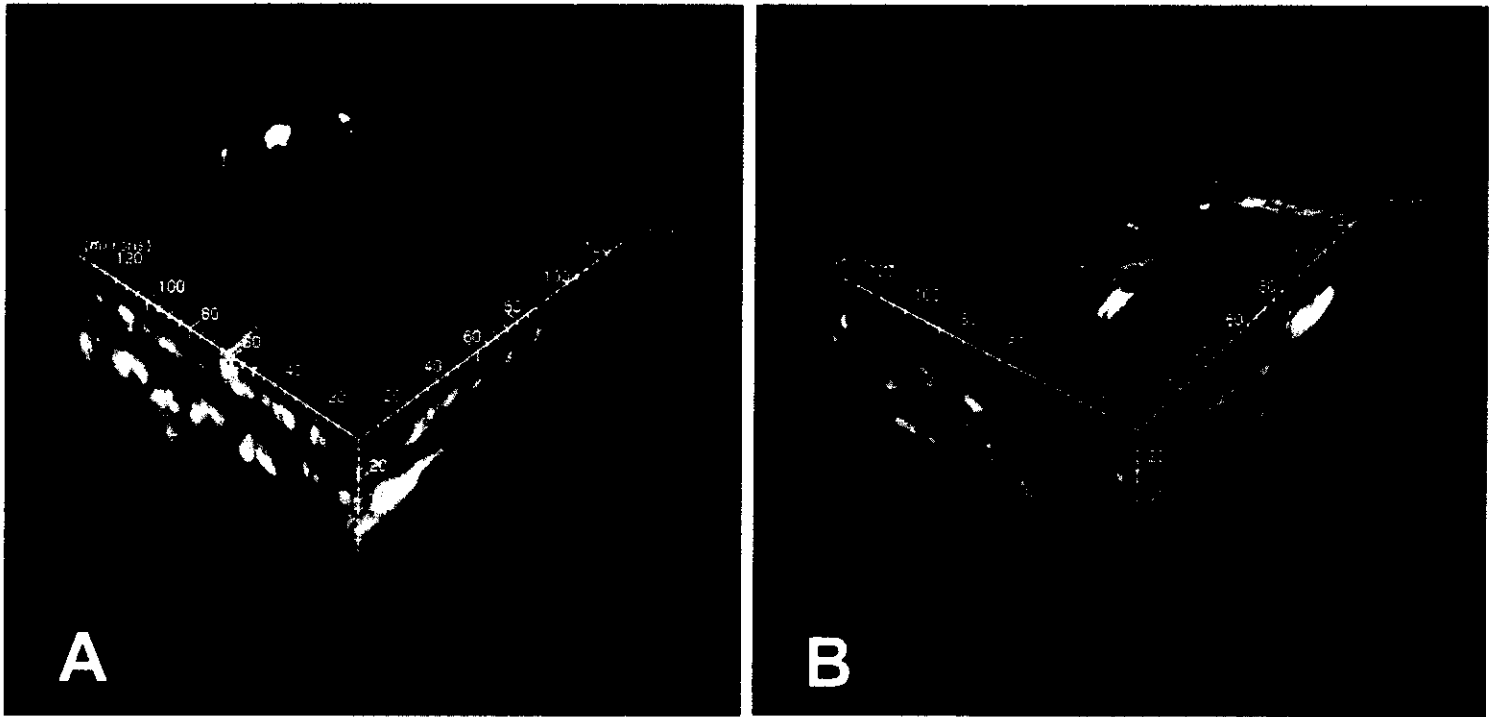
Fig. 4 3-D reconstructed multiphoton images demonstrating autofluorescence of a tissue-derived ECM biomaterial, small intestinal submucosa, sectioned optically from luminal (A) or abluminal (B) surfaces.
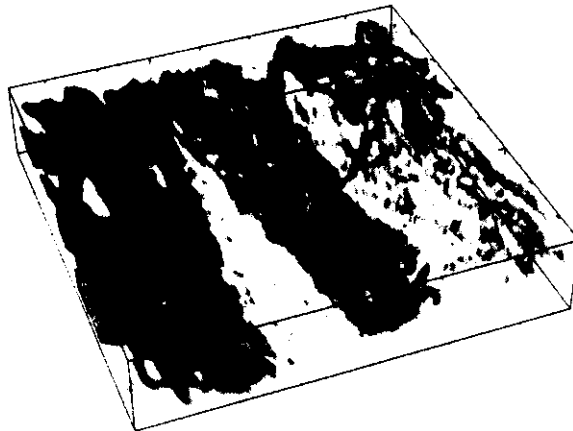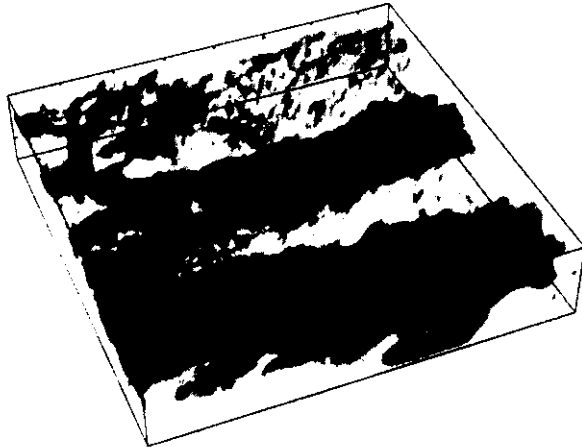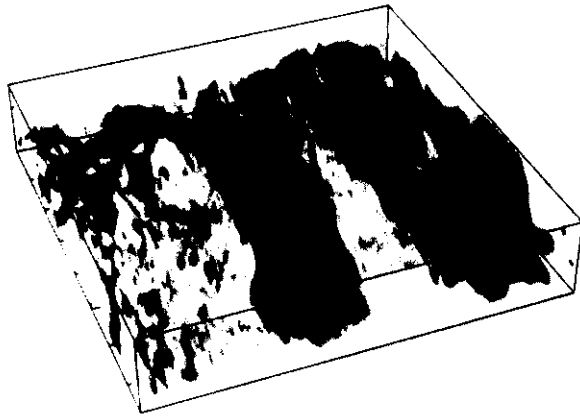
Fig. 5 3-D reconstructed confocal images of cells growing on and within a tissue-derived ECM substrate. small intestinal submucosa. Components of the ECM substrate were imaged based on their autofluorescence properties. and cell nuclei were stained with Hoechst 33342. (See color plates.)

niques to study collagen fibrillogenesis and ECM assembly, structural aspects of
ECM-based biomaterials, as well as cell interactions within 3-D matrices (e.g.,
migration). New insights provided by these techniques regarding ECM and
ECM–cell signaling will further the understanding of tissue structure and function
and contribute to the development of new and improved strategies for tissue
repair, replacement, and maintenance.

References

Aslund, N., and Liljeborg, A. (1992). A method to extract homogeneous regions in 3-D confocal microscopy enabling compensation for depth dependent light attenuation. *Micron Microsc. Acta* **23,** 463–479.

Bissell, M. J., Hall, H. G., and Parry, G. (1982). How does the extracellular matrix direct gene expression? *J. Theor. Biol.* **99,** 31–68.

Boyde, A., and Jones, S. J. (1995). Mapping and measuring surfaces using reflection confocal micros-copy. *In* "Handbook of Biological Confocal Microscopy" (J. B. Pawley, ed.), pp. 255–266. Plenum, New York.

Brakenhoff, G. J., Blom, P., and Barends, P. J. (1979). Confocal scanning light microscopy with high aperture immersion lenses. *J. Microsc.* **117,** 219.

Brakenhoff, G. J., van der Voort, H., van Spronsen, E., and Nanninga, N. (1988). 3-dimensional imaging of biological structures by high resolution confocal scanning laser microscopy. *Scanning Microsc.* **2,** 33–40.

Brennan, M. (1989). Changes in solubility, non-enzymatic glycation, and fluorescence of collagen in tail tendons from diabetic rats. *J. Biol. Chem.* **264,** 20947–20952.

Brightman, A. O., Rajwa, B. P., Sturgis, J. E., McCallister, M. E., Robinson, J. P., and Voytik-Harbin, S. L. (2000). Time-lapse confocal reflection microscopy of collagen fibrillogenesis and ECM assembly *in vitro. Biopolymers,* in press.

Centonze, V. E., and White, J. G. (1998). Multiphoton excitation provides optical sections from deeper within scattering specimens than confocal imaging. *Biophys. J.* **75,** 2015–2024.

Deckelbaum, L. I., Lam, J. K., Cabin, H. S., Clubb, K. S., and Long, M. B. (1987). Discrimination of normal and atherosclerotic aorta by laser-induced fluorescence. *Lasers Surg. Med.* **7,** 330–335.

Denk, W., Strickler, J., and Webb, W. W. (1990). Two-photon laser scanning fluorescence microscopy. *Science* **248,** 73–76.

Engel, J., (1994). Electron microscopy of extracellular matrix components. *Methods Enzymol.* **245,** 469–488.

Engel, J., and Furthmayr, H. (1987). Electron microscopy and other physical methods for the charac-terization of extracellular matrix components: Laminin, fibronectin, collagen IV, collagen VI, and proteoglycans. *Methods Enzymol.* **145,** 3–78.

Frank, J. (1992). "Electron Tomography." Plenum, New York..

Friedl, P., Maaser, K., Klein, C. E., Niggemann, B., Krohne, G., and Zanker, K. S. (1997). Migration of highly aggressive MV3 melanoma cells in 3-dimensional collagen lattices results in local matrix reorganization and shedding of $\alpha2$ and $\beta1$ integrins and CD44. *Cancer Res.* **57,** 2061–2070.

Goeppert-Mayer, M. (1931). Ueber elementarakte mit quantenspruengen. *Ann. Phys.* **9,** 273–294.

Gunzer, M., Kampgen, E., Brocker, E., Zanker, K. S., and Friedl, P. (1997). Migration of dendritic cells in 3D-collagen lattices. Visualisation of dynamic interactions with the substratum and the distribution of surface structures via a novel confocal reflection imaging technique. *In* "Dendritic Cells in Fundamental and Clinical Immunology" (P. Ricciardi-Castagnoli, ed.), pp. 97–103. Plenum, New York.

Hell, S., Reiner, G., Cremer, C., and Stelzer, E. H. K. (1993). Aberrations in confocal fluorescence microscopy induced by mismatches in refractive index. *J. Microsc.* **169,** 391–405.

Holmes, T. J., Bhattacharyya, S., Cooper, J. A., Hanzel, D., Krishnamurthi, V., Lin, W.-C., Roysam, B., Szarowski, D. H., and Turner, J. N. (1995). Light microscopic images reconstructed by maximum likelihood deconvolution. *In* "Handbook of Biological Confocal Microcopy" (J. B. Pawley, ed.), pp. 389–402. Plenum, New York.

Kollias, N., Gillies, R., Moran, M., Kochevar, I. E., and Anderson, R. R. (1998). Endogenous skin fluorescence includes bands that may serve as quantitative markers of aging and photoaging. *J. Invest. Dermatol.* **111**, 776–780.

Leffell, D. J., Stetz, M. L., Milstone, L. M., and Deckelbaum, L. I. (1988). In vivo fluorescence of human skin: A potential marker of photoaging. *Arch. Dermatol.* **124**, 1514–1518.

Messerli, J. M., and Perriard, J.-C. (1995). Three-dimensional analysis and visualization of myofibrillogenesis in adult cardiomyocytes by confocal microscopy. *Microsc. Res. Technol.* **30**, 521–530.

Oldenbourg, R., Terada, H., Tiberio, R., and Inoue, S. (1993). Image sharpness and contrast transfer in coherent confocal microscopy. *J. Microsc.* **172**, 31–39.

Potter, S. M. (1996). Vital imaging: Two photons are better than one. *Curr. Biol.* **6**, 1595–1598.

Robinson, J. P., Brightman, A. O., Kelley, S., Rajwa, B., Sturgis, J., and Voytik-Harbin, S. L. (1999). Imaging technique for kinetic evaluation of collagen matrix assembly. *FASEB J.* **13**, A344 (Abstract).

Schomacker, K. T., Frisoli, J. K., Compton, C. C., Flotte, T. J., Richter, J. M., Nishioka, N. S., and Deutsch, T. F. (1992). Ultraviolet laser-induced fluorescence of colonic tissue: Basic biology and diagnostic potential. *Lasers Surg. Med.* **12**, 63–78.

Semler, E. J., Tjia, J. S., and Moghe, P. V. (1997). Analysis of surface microtopography of biodegradable polymer matrices using confocal reflection microscopy. *Biotechnol. Prog.* **13**, 630–634.

Shaw, P. J. (1995). Comparison of wide-field/deconvolution and confocal microscopy for 3D imaging. *In* "Handbook of Biological Confocal Microscopy" (J. B. Pawley, ed.), pp. 373–387. Plenum, New York.

Sheppard, C. J. R. (1987). Scanning optical microscopy. *In* "Advances in Optical and Electron Microscopy" (E. Barer and V. E. Cosslett, eds.), pp. 1–98. Academic Press, London.

Sturgis, J. E., Robinson, J. P., and Voytik-Harbin, S. L. (1998). Three-dimensional (3D) culture of human vascular cells in a complex extracellular matrix (ECM). *Mol. Biol. Cell* **9**(Suppl.), 168a [Abstract].

Visser, T. D., Groen, F. C. A., and Brakenhoff, G. J. (1991). Absorption and scattering correction in fluorescence confocal. *J. Microsc.* **163**, 189–200.

Voytik-Harbin, S. L., Brightman, A. O., Waisner, B. Z., Robinson, J. P., and Lamar, C. H. (1998a). Small intestinal submucosa: A tissue-derived extracellular matrix that promotes tissue-specific growth and differentiation of cells *in vitro. Tissue Eng.* **4**, 157–174.

Voytik-Harbin, S. L., Rajwa, B. P., Sturgis, J. E., McCallister, M. E., Brightman, A. O., and Robinson, J. P. (1998b). Time-lapse confocal reflection (TLR) imaging for the study of extracellular matrix assembly. *Mol. Biol. Cell* **9**(Suppl.), 61a(Abstract).

Wijnaendts van Resandt, R. W., Marsman, H. J. B., Kaplan, R., Davoust, J., Stelzer, E. K. H., and Stricker, R. (1985). Optical fluorescence microscopy in 3 dimensions: Microtomoscopy. *J. Microsc.* **138**, 29–34.

Wokosin, D. L., and White, J. G. (1997). Optimization of the design of a multiple-photon excitation laser scanning fluorescence imaging system. Three Dimensional Microscopy: Imaging Acquisition and Processing IV. *Proc. SPIE* **2984**, 25–29.

Wokosin, D. L., Centonze, V. E., White, J. G., Armstrong, D., Robertson, G., and Ferguson, A. I. (1996). All-solid-state ultrafast lasers facilitate multiphoton excitation fluorescence imaging. *IEEE J. Select. Top. Quant. Elec.* **2**, 1051–1065.